Drosophila Mgr, a Prefoldin subunit cooperating with von Hippel Lindau to regulate tubulin stability

Nathalie Delgehyr[a,1,2], Uta Wieland[a,1], Hélène Rangone[a], Xavier Pinson[a,3], Guojie Mao[a,4], Nikola S. Dzhindzhev[a], Doris McLean[a,5], Maria G. Riparbelli[b], Salud Llamazares[c], Giuliano Callaini[b], Cayetano Gonzalez[c], and David M. Glover[a,6]

[a]Department of Genetics, Cancer Research United Kingdom Cell Cycle Genetics Research Group, University of Cambridge, Cambridge CB2 3EH, United Kingdom; [b]Department of Evolutionary Biology, University of Siena, Siena I-53100, Italy; and [c]Cell Division Group, Institut de Recerca Biomedica, Barcelona 08028, Spain

Edited by Yixian Zheng, Carnegie Institution of Washington, Baltimore, MD, and accepted by the Editorial Board February 23, 2012 (received for review May 31, 2011)

Mutations in *Drosophila merry-go-round (mgr)* have been known for over two decades to lead to circular mitotic figures and loss of meiotic spindle integrity. However, the identity of its gene product has remained undiscovered. We now show that *mgr* encodes the Prefoldin subunit counterpart of human von Hippel Lindau binding-protein 1. Depletion of Mgr from cultured cells also leads to formation of monopolar and abnormal spindles and centrosome loss. These phenotypes are associated with reductions of tubulin levels in both *mgr* flies and *mgr* RNAi-treated cultured cells. Moreover, *mgr* spindle defects can be phenocopied by depleting β-tubulin, suggesting Mgr function is required for tubulin stability. Instability of β-tubulin in the *mgr* larval brain is less pronounced than in either *mgr* testes or in cultured cells. However, expression of transgenic β-tubulin in the larval brain leads to increased tubulin instability, indicating that Prefoldin might only be required when tubulins are synthesized at high levels. Mgr interacts with *Drosophila* von Hippel Lindau protein (Vhl). Both proteins interact with unpolymerized tubulins, suggesting they cooperate in regulating tubulin functions. Accordingly, codepletion of Vhl with Mgr gives partial rescue of tubulin instability, monopolar spindle formation, and loss of centrosomes, leading us to propose a requirement for Vhl to promote degradation of incorrectly folded tubulin in the absence of functional Prefoldin. Thus, Vhl may play a pivotal role: promoting microtubule stabilization when tubulins are correctly folded by Prefoldin and tubulin destruction when they are not.

folding | chaperone | Gim | E3 ubiquitin ligase

Eukaryotes have a complex molecular machinery that promotes the folding and assembly of the actin and tubulin subunits of microfilaments and microtubules (MTs). Several protein complexes and ancillary proteins are involved in assembling αβ-tubulin dimers: chaperonin containing tailless protein (CCT), the prefoldin complex, phosducin-like CCT regulatory proteins, and five cofactors [reviewed by Lundin et al. (1)]. Prefoldin is a hexameric protein complex (2) thought to bind to partially folded tubulin and actin molecules from the ribosome (3–5).

One component of the prefoldin complex also interacts with the tumor suppressor Von Hippel Lindau (Vhl) protein and is known as Von Hippel Lindau binding protein 1 (VBP1) (6). The Vhl protein is a multifunctional adapter protein that influences multiple transcriptional pathways (for review, see refs. 7 and 8), as well as the functions of the collagen IV and fibronectin extracellular matrix and MTs. Its best-characterized function is in a complex with Cullin2 as an E3 ubiquitin-protein ligase that targets hypoxia-inducible factor α (HIF1α) for destruction (9, 10). Vhl interacts with the CCT to mediate the formation of the Vhl-ElonginB/C-Cullin2 complex (VBC) (11–15). Therefore, the interaction between Vhl and the prefoldin complex could be relevant for the folding of the VBC. However, Vhl also interacts with cytoplasmic MTs: in mitosis to influence spindle orientation (16) and in interphase to inhibit catastrophe and promote rescue (17, 18). Such an effect could account for the role of Vhl in stabilizing MTs in *Drosophila* follicle cells to maintain the integrity of this epithelium (19). Vhl is also required with the GSK-3β protein kinase to maintain the stability of the ciliary axoneme (20–22).

Genetic studies first identified prefoldin in yeast through mutants that could still fold tubulin but more slowly (hence the name GIM: genes involved in microtubule biogenesis) (23). Loss of prefoldin in *Caenorhabditis elegans* is lethal because of a high demand for tubulin in mitotic cells in the embryo (24). In plants, prefoldin 6 has been shown to be required for normal MT dynamics and organization (25). Knockout of *Prefoldin 1* or mutation in *Prefoldin 5* of mice lead to a variety of defects characteristic of tubulin functions in cilia or in the CNS (26, 27).

We now identify *merry-go-round* (*mgr*), a *Drosophila* gene identified over two decades ago, as encoding the prefoldin 3 (Pfdn3)/VBP1/Gim2 subunit. We show that the characteristic monopolar mitotic spindles of this mutant arise because of diminished levels of tubulin subunits. We also show that *mgr* mutants cannot stabilize tubulin following overexpression of a tubulin transgene. Finally, our studies show that Mgr can physically interact with Vhl. Moreover, depletion of Vhl rescues the destabilization of tubulin resulting from loss of Mgr. This finding leads us to suggest that the E3 ubiquitin-protein ligase properties of Vhl may be required for the degradation of incorrectly folded tubulin, suggesting that Vhl can also contribute to MT dynamics through the regulation of tubulin degradation.

Results

Mgr Is a Subunit of the Highly Conserved Gim Complex/Prefoldin. The *mgr* gene was originally recovered as an X-ray–induced mutant resulting in lethality late in development associated with circular mitotic figures in larval neuroblasts (28). We confirmed this phenotype by immunostaining the CNS to reveal MTs and centrosomal antigens in several mutant alleles of *mgr* and by counting proportions of cells at different stages of mitosis (Fig. 1 *A* and *B*,

Author contributions: N. Delgehyr, U.W., D.M., C.G., and D.M.G. designed research; N. Delgehyr, U.W., H.R., X.P., G.M., N. Dzhindzhev, D.M., M.R., S.L., and G.C. performed research; N. Delgehyr, U.W., G.M., and N. Dzhindzhev contributed new reagents/analytic tools; N. Delgehyr, U.W., H.R., X.P., D.M., M.R., S.L., G.C., C.G., and D.M.G. analyzed data; and N. Delgehyr, C.G., and D.M.G. wrote the paper.

The authors declare no conflict of interest.

This article is a PNAS Direct Submission. Y.Z. is a guest editor invited by the Editorial Board.

[1]N. Delgehyr and U.W. contributed equally to this work.

[2]Present Address: Institut de Biologie de l'Ecole Normale Supérieure, Laboratory of Cilia Biology and Neurogenesis, 75005 Paris, France.

[3]Present Address: Institut de Recherche en Immunologie et en Cancérologie, Université de Montréal, Montréal, QC, Canada H3C 3J7.

[4]Present Address: Huntingdon Life Sciences, Alconbury, Huntingdon, Cambridgeshire PE28 4HS, United Kingdom.

[5]Present Address: CXR Biosciences Ltd., Dundee DD1 5JJ, Scotland, United Kingdom.

[6]To whom correspondence should be addressed. E-mail: d.glover@gen.cam.ac.uk.

This article contains supporting information online at www.pnas.org/lookup/suppl/doi:10.1073/pnas.1108537109/-/DCSupplemental.

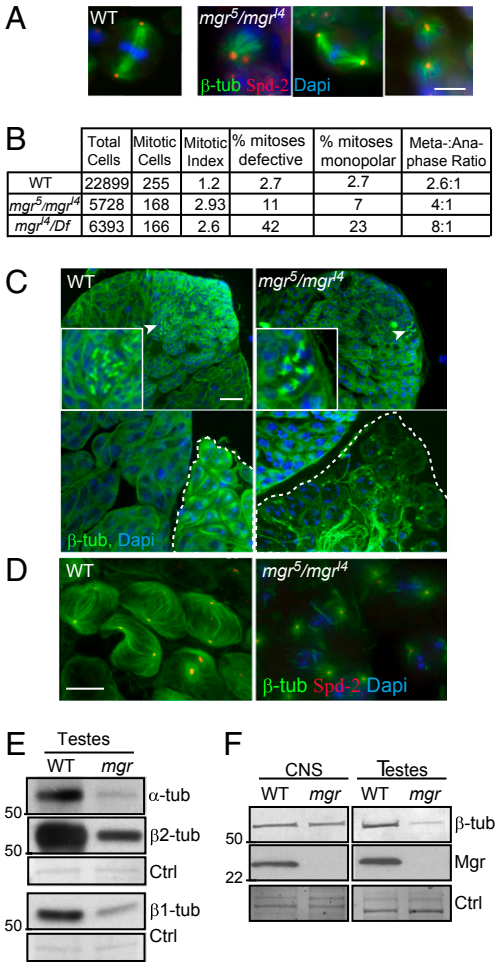

	Total Cells	Mitotic Cells	Mitotic Index	% mitoses defective	% mitoses monopolar	Meta-:Ana-phase Ratio
WT	22899	255	1.2	2.7	2.7	2.6:1
mgr^5/mgr^{14}	5728	168	2.93	11	7	4:1
mgr^{14}/Df	6393	166	2.6	42	23	8:1

Fig. 1. The *mgr* mutant flies have microtubule-based abnormalities. (*A*) Representative mitotic spindles from squashed preparations of wild-type (*Oregon R*) and *mgr* (mgr^5/mgr^{14}) mutant third-instar larval brains stained to reveal microtubules (β-tubulin, green), centrosome (Spd-2, red), and DNA (Dapi, blue). (*Right column, Left* and *Right*) Images of *mgr* neuroblasts show examples of monopolar spindles; (*Center*) a bipolar spindle of abnormal morphology. (Scale bar, 5 μm.) (*B*) Table indicating the mitotic defects observed in wild-type, mgr^5/mgr^{14} (compared with wild-type, mitotic defects $P = 0.001$; monopolar spindles $P = 0.021$), and mgr^{14}/Df (compared with wild-type $P < 0.0001$ for both mitotic defects and monopolar spindles); *P* values from χ^2 analysis. Mitotic defects comprised monopolar and disorganized spindles (at least five independent brains scored). (*C*) Testes from wild-type and *mgr* (mgr^5/mgr^{14}) mutant flies stained to reveal microtubules (β-tubulin, green) and DNA (Dapi, blue). (Scale bar, 10 μm.) (*Upper*) Young cysts (spermatogonia) in the apical region: arrowheads indicate mitotic cysts, shown in the *Inset* at 3× magnification; (*Lower*) Late primary spermatocytes with impaired microtubule network particularly in meiosis (compare outlined cysts). (*D*) Meiosis I spindles from wild-type and *mgr* stained to reveal microtubules (β-tubulin, green), centrosomes (Spd-2, red), and DNA (Dapi, blue). (Scale bar, 10 μm.) Of the meiotic spindles observed in *mgr* mutant testes, 100% were abnormal compared with wild-type where no abnormalities were observed (at least five testes scored and >208 complete cysts observed, *P* value from Student *t* test < 0.0001). (*E*) Western blots of the ubiquitous α- and β1-tubulin and the testes specific β2-tubulin isoform in testes protein extracts from wild-type and *mgr* mutant flies, showing that all three tubulin levels are reduced in *mgr* mutants. Amido black staining is the loading control (Ctrl). (*F*) Western blot of β-tubulin and Mgr in wild-type and *mgr* CNS and testes protein extracts, showing the absence of Mgr and the differential depletion of tubulin according to the tissue. Amido black staining is the loading control (Ctrl).

and Fig. S1 *A* and *B*). The prometaphase-like cells in such preparations could have bipolar spindles that may lack one or both centrosomes or monopolar spindles having one or two centrosomes at the single pole (Fig. 1*A* and Fig. S1 *A* and *B*). These centrosomes were positive for several known *Drosophila* centrosomal antigens (Fig. S1*B*). The mitotic index was elevated some twofold over that in wild-type larval brains and the ratio of metaphase:anaphase figures was elevated by two- to threefold over wild-type, depending upon the allelic combination (Fig. 1*B*). Taken together, these data are indicative of a delay in progression through the mitotic cycle. Previous phase-contrast images of spermatocytes of *mgr* mutants suggested the absence of meiotic spindles (28). To determine whether this suggestion was correct, we used an antibody recognizing both the β1-tubulin isoform and the β2-tubulin male germ-line–specific isoform to immunostain the testes of mgr^{14}/mgr^5 transheterozygotes, a strong hypomorphic mutant combination that shows pharate lethality but gives some sterile adults. This process revealed that mgr^{14}/mgr^5 had sufficient MTs to permit the premeiotic mitosis (arrowheads and magnification in Fig. 1*C*). However, mature (white dashed outlined cysts) but not young primary spermatocyte cysts had reduced MTs (Fig. 1*C* and Fig. S1*C*) such that the meiotic spindles were either absent or highly abnormal (Fig. 1*D*). Western blotting with antibodies specific for α-tubulin, β1-tubulin, and β2-tubulin (29) showed that the levels of all three tubulins were reduced in mgr^{14}/mgr^5 mutant testes (Fig. 1*E*), thus accounting for the spindle defects.

To understand why reduction in levels of the *mgr* gene product might have such an effect on tubulin levels, we set out to identify the *mgr* gene product. Small deficiencies [*Df(3R)thoR1*, *Df(3R)pros235*, and *Df(3R)pros640*] (30), which each fail to complement *mgr*, placed the *mgr* gene to 86E4 in a region containing 14 predicted genes (Fig. S2 *A* and *B*). Using a combination of RNAi to identify mitotic phenotypes resulting from the knockdown of each of these genes (Fig. S2 *C–F*) together with the sequencing of candidate genes from chromosomes carrying *mgr* mutant alleles, we identified the predicted gene *CG6719* as *mgr*. We confirmed its identity by showing that lethality of mgr^{14}/mgr^1 mutant, a combination showing pharate lethality, could be rescued with a *CG6719* transgene. In addition to the mitotic phenotype, RNAi-mediated knockdown of *mgr* led to a reduction of cytoplasmic MTs in interphase cells (Fig. S2*G*).

Sequencing of the *mgr* mutant alleles revealed them to represent a variety of deletion, frame-shift, and nonsense mutations (Fig. S2*H* and *SI Materials and Methods*). In this study we focused on two mutant alleles: mgr^{14}, a null mutant having a deletion in the 5′UTR; and mgr^5, which because of a nonsense mutation, produces a truncated protein (not detectable by Western blot) and additionally carries a 41-bp deletion in its 3′UTR. Immunostaining on wild-type cells using the anti-Mgr antibody we generated showed that the protein localizes throughout the cytoplasm in testis, brain, and cultured cells at all cell-cycle stages (Fig. S3). Western blots on protein extracts of testes and larval CNS confirmed that the protein was not detectable in mgr^{14}/mgr^5 mutants (Fig. 1*F*). The sequence of *mgr* revealed it to encode a subunit of the Gim/prefoldin complex; Mgr shows 37% amino acid identity with its yeast homolog PAC10 and 57% with its human homolog VBP1/Pfdn3/Gim2. Thus, the phenotypes of *mgr* mutants would be consistent with the improper folding and degradation of tubulin in the absence of the Prefoldin complex. The greater reductions in tubulin levels in the testes than in the CNS would account for the stronger phenotype in the spermatocytes (Fig. 1*F*).

Spindle Abnormalities Result from Tubulin Destabilization Following Mgr Depletion. To gain further insight into how Mgr depletion affects spindle formation, we turned to RNAi in the DMEL-2 *Drosophila* cell line (Fig. 2). Transfection with *mgr* dsRNA for 6 d increased the proportion of cells with monopolar spindles similar in appearance to those seen in *mgr* mutant neuroblasts and greatly above the background level of mitotic abnormalities typical of this cell line (Fig. 2 *A* and *B*). Further cycles of *mgr*

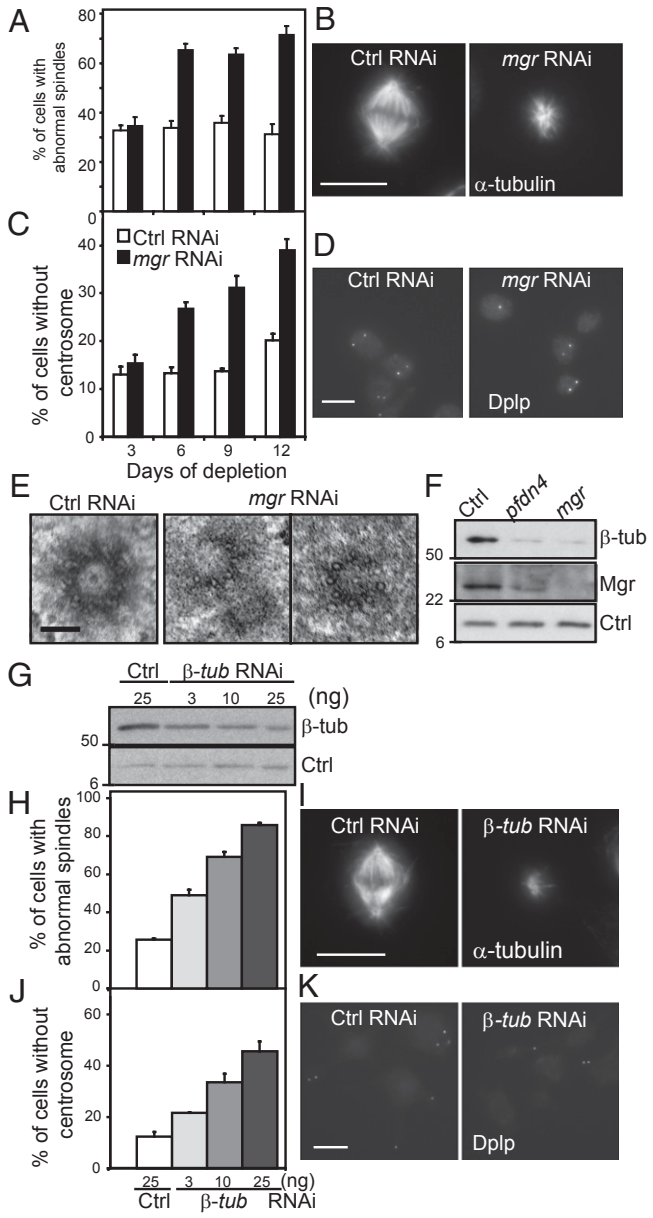

Fig. 2. Mgr or partial β-tubulin depletion result in similar microtubule-based abnormalities. DMEL-2 cells transfected with control (Ctrl) or *mgr* dsRNA for 3-d intervals up to a maximum of 12 d (*A*–*F*). (*A*) Percentage of prometaphase and metaphase cells with monopolar or disorganized spindles scored following immunostaining, as in *B*. Error bars = SEMs for more than three independent experiments; $n > 150$ metaphase cells. (*B*) Cells immunostained to reveal microtubules (α-tubulin) 6 d after transfection. (Scale bar, 10 μm.) (*C*) Percentage of cells without centrosomes scored after immunostaining, as in *D*. Error bars = SEMs of more than five independent experiments; $n > 1{,}000$ cells. (*D*) Cells immunostained to reveal centrosomes (Dplp) 6 d after transfection. (Scale bar, 10 μm.) (*E*) Electron micrographs of centrioles in control cells (Ctrl RNAi) and following 9–12 d of *mgr* RNAi. Twenty-percent of the centrioles showed an abnormal structure after Mgr depletion, whereas none were observed in the control depletion ($n = 10$). (Scale bar, 0.1 μm.) (*F*) Western blot of β-tubulin, Mgr and H2A (loading control, Ctrl) 6 d after transfection with *mgr*, *pfdn4*, or control dsRNAs. (*G*–*K*) DMEL-2 cells treated with a range of concentrations (3, 10, and 25 ng/mL) of β-tubulin dsRNA for 6 d. (*G*) Western blot of β-tubulin and H2A (loading control, Ctrl) following such treatment. (*H*) Proportion of prometaphase and metaphase cells with monopolar or disorganized spindles in relation to β-*tubulin* dsRNA treatment. Error bars = SEMs of more than two independent experiments; $n > 100$ metaphase cells. (*I*) Cells labeled with an anti-α-tubulin to reveal spindle microtubules in control and β-*tubulin* dsRNA treated cells. (Scale bar 10 μm.) (*J*) Percentage of cells without centrosomes in relation to β-*tubulin* dsRNA treament. Error bars = SEMs of more than two independent experiments; $n > 200$ cells. (*K*) Cells labeled to reveal centrosomes (Dplp) following control dsRNA and β-*tubulin* dsRNA treatment. (Scale bar, 10 μm.)

RNAi did not lead to any significant further increase in spindle abnormalities such that after 12 d, some 60% of mitotic cells had monopolar or disorganized spindles. Codepletion of BubR1 or Mad2 and Mgr led to a decrease of abnormal spindles and a restoration of a normal mitotic index compared with mgr RNAi alone (Fig. S4). These results suggest that cells are delayed in mitotic progression after Mgr depletion in response to the spindle assembly check point. To determine whether spindle abnormalities were related to centrosome defects, we counted $Dplp^+$ punctae in interphase cells after the same period of Mgr depletion. This process revealed a progressive loss of centrosomes from cells lagging behind the appearance of spindle defects such that 40% of cells had no centrosomes by day 12 (Fig. 2 *C* and *D*). This lag in the loss of centrosomes could be because of either or both defects in centrosome duplication or segregation as a consequence of the spindle defects. To address whether Mgr depletion affected centriole structure, we carried out electron microscopy, which revealed abnormalities typical of centriole duplication/formation defects; 20% of the centrioles were incomplete and composed of singlet MTs rather than doublets or triplets, as in control cells (Fig. 2*E*).

Immunoblotting revealed that Mgr depletion led to a reduction in β-tubulin levels by ∼70% (Fig. 2*F*), also apparent by immunofluorescence (Fig. S2*G*). Depletion of the Pfdn4 Prefoldin subunit also led not only to a similar reduction in β-tubulin, but also in Mgr levels, indicating the importance of interactions between subunits of the complex for its stability. Levels of γ-tubulin were reduced by ∼50%, whereas actin was unaffected (Fig. S5 *A* and *B*). To determine whether the spindle and centrosome defects resulting from Mgr depletion might reflect the reduction in tubulin levels, we performed partial depletion of β- and γ-tubulin (Fig. 2 *G*–*K* and Fig. S5 *C*–*J*). DMEL-2 cells were treated with varying amounts of β- or γ-tubulin dsRNA and assayed for spindle defects and centrosome numbers after 6 d. An increase in monopolar and disorganized spindles and in centrosome loss mirrored the extent of β- and γ-tubulin knockdown. However, only the β-tubulin knockdown recapitulated the small spindle size observed after *mgr* RNAi (Fig. S5*D*). Moreover, γ-tubulin knockdown leads to a population of bipolar spindles with the centrosomes at one pole only (Fig. S5*E*), which was not observed after *mgr* RNAi or partial depletion of β-tubulin. Thus, the mitotic defects that follow loss of Mgr appear to be largely a consequence of tubulin destabilization. To assess if the structural defects observed on the centrioles after *mgr* RNAi was a consequence of αβ- or γ-tubulin depletion, we carried out electron microscopy in cells partially depleted for 6 d for β- or γ-tubulin. These analyses failed to reveal any centriolar structural defects in either case (Fig. S5 *I* and *J*). However, the difficulties in assessing the level and timing of β- or γ-tubulin depletion that would be equivalent to that seen following *mgr* RNAi, together with the restricted numbers of centrioles that can be observed by electron microscopy in such experiments, makes it difficult to reach a firm conclusion about the effects on centrioles.

Levels of Free αβ-Tubulin Sensitize Mgr Activity. The above studies showed that MTs of different tissues present different sensitivity to reduced Mgr levels (Fig. 1). Moreover, even in *mgr* testes, where disruption of the MT network is most pronounced, it only occurs once primary spermatocytes have reached a late stage in their development. This result is despite the fact that Mgr pro-

tein is present throughout the wild-type testes and so ought, in principle, to be equally functional at all stages. This finding suggests that the onset of synthesis of the β2-tubulin testes specific isoform in late spermatogenesis might bring a particular requirement for Mgr (31, 32). If this were the case, we wondered whether increased synthesis of β1-tubulin from a transgene might trigger a stronger requirement for Mgr in larval neuroblasts (Fig. 3). We found that in mgr^{l4}/mgr^{5} mutant neuroblasts the level of endogenous β-tubulin was only slightly reduced (by 25% compared with wild-type levels). The additional expression of β1-tubulin–GFP did not drastically affect endogenous β-tubulin levels if one wild-type copy of *mgr* was present ($mgr^{5}/+$;*β1-tubulin–GFP*, a reduction of 15% compared with wild-type). However, in mgr^{l4}/mgr^{5} mutants, expression of β1-tubulin–GFP leads to a further decrease in levels of endogenous β-tubulin by 60% compared with wild-type levels (Fig. 3 *A* and *B*). There was also a dramatic loss of MT staining in immunostained preparations of the larval CNS of such organisms (Fig. 3*C*). Taken together, these results suggest that if tubulin levels exceed a certain threshold, this overproduced tubulin may change the complex balance of folding, causing a synthetically lethal phenotype with *mgr*.

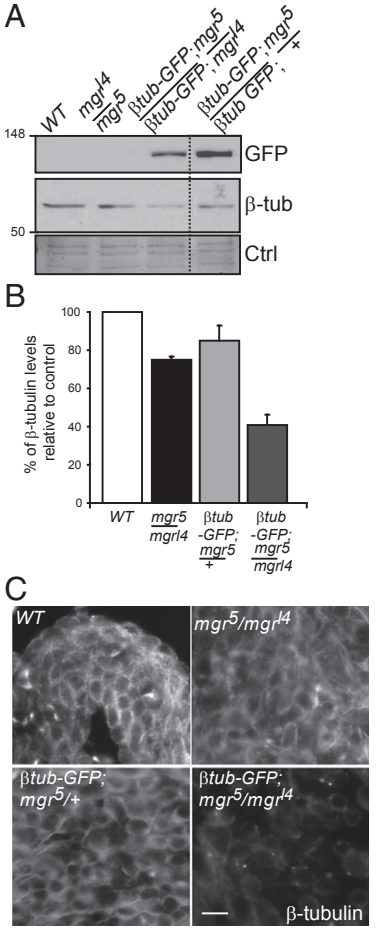

Fig. 3. Mgr is a sensor of a free pool of tubulin. (*A*) Western blot of GFP or endogenous β-tubulin in extracts of testes of wild-type or mgr^{l4}/mgr^{5} flies in presence or absence of an exogenous GFP-tagged β1-tubulin transgene. Note the β1-tubulin-GFP is not detected by the β-tubulin antibody due to low levels of expression. Amido black staining is loading control (Ctrl). (*B*) Quantitation of the endogenous β-tubulin levels relative to the wild-type control on Western blots. Error bars = SEMs for two independent experiments. (*C*) Wild-type field images of brain squashes from indicated genotypes stained to reveal microtubules (β-tubulin). (Scale bar, 5 μm.)

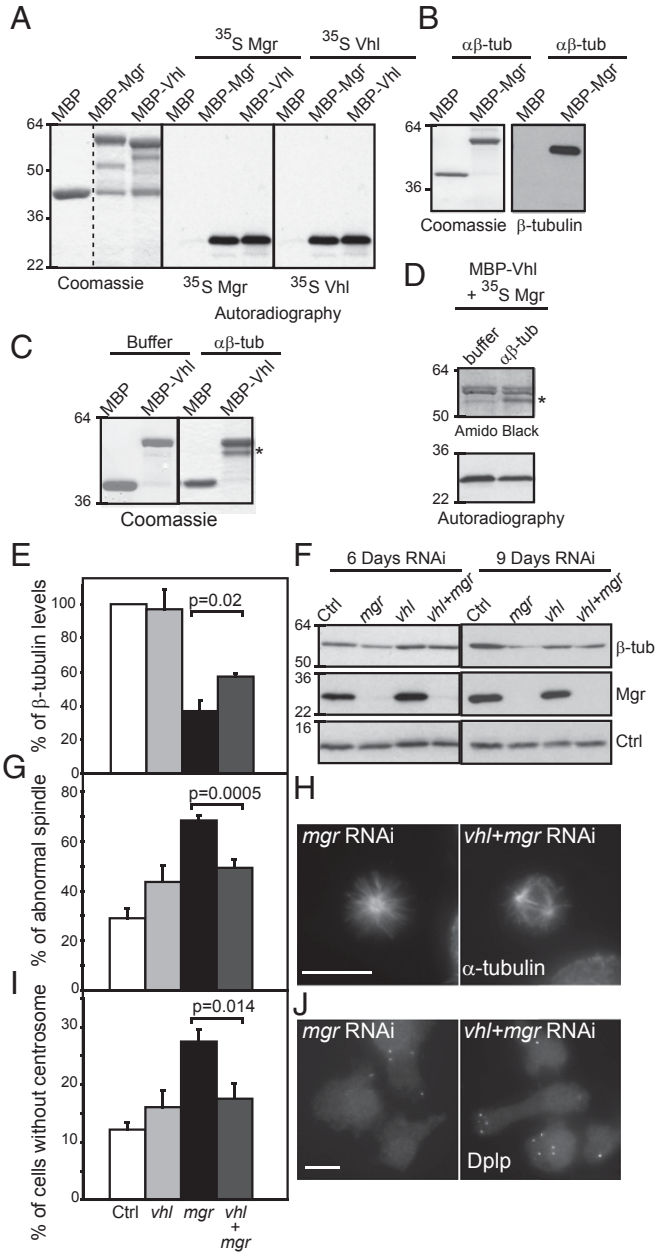

Fig. 4. Mgr and Vhl cooperate in regulating tubulin destruction. (*A*) MBP, MBP-Mgr, and MBP-Vhl, affinity purified from *Escherichia coli* extracts (Coomassie stain) tested for binding ^{35}S-Methionine labeled Mgr and Vhl synthesized by coupled transcription-translation in vitro (Autoradiography). (*B*) MBP and MBP-Mgr, affinity-purified from *E. coli* extracts (Coomassie stain) tested for binding purified αβ-tubulin (Western blot). (*C*) MBP and MBP-Vhl, affinity-purified from *E. coli* extracts (Coomassie stain, *Right*) tested for binding-purified αβ-tubulin (Coomassie stain, *Left*). (*D*) MBP-Vhl, affinity purified from *E. coli* extracts, and tested for binding ^{35}S-Mgr (as in *A*). Excess of purified αβ-tubulin is insufficient to release the Vhl:Mgr interaction. (*E–J*) DMEL-2 cells treated with Control, *mgr*, *Vhl*, or *mgr* and *Vhl* dsRNA for 6 or 9 d. (*E*) Levels of β-tubulin in three independent experiments 9 d after transfection. (*F*) Western blot of β-tubulin and Mgr after such treatment. H2A is used as loading control (Ctrl). (*G*) Percentage of prometaphase and metaphase cells with monopolar or disorganized spindles after indicated dsRNA treatment. Error bars = SEMs of three independent experiments. $n > 300$ metaphase cells; (*H*) Mitotic cells immunostained to reveal microtubules (α-tubulin). (Scale bar, 10 μm.) (*I*) Percentage of cells without centrosome 9 d after indicated transfections. Error bars = SEM of three independent experiments. $n > 600$ cells. (*J*) Cells immunostained to reveal centrosomes (Dplp). (Scale bar, 10 μm.) All *P* values are from Student *t* tests.

Mgr and Vhl Cooperate to Control the Degradation of αβ-Tubulins. Mgr's human counterpart, which shares 57% amino acid identity, can interact with human Vhl, an E3 ubiquitin-protein ligase also able to bind the MT lattice (17). Several lines of evidence indicated that Mgr was able to interact with *Drosophila* Vhl and that both proteins could interact with tubulin monomers and dimers. First, beads carrying Maltose binding protein (MBP)-Mgr or MBP-Vhl fusion proteins synthesized in bacteria could bind ^{35}S-labeled Mgr or Vhl synthesized by coupled transcription-translation in vitro (Fig. 4*A*). This experiment also indicated that both proteins could undertake self-self interactions. Second, both Mgr and Vhl synthesized in bacteria were able to bind ^{35}S-labeled β1-tubulin synthesized by coupled transcription-translation in vitro (Fig. S6 *A* and *B*). Conversely β1-tubulin synthesized in bacteria would interact with ^{35}S-labeled Vhl or Mgr (Fig. S6 *C* and *D*). Third, MBP-tagged Mgr or MBP-tagged Vhl immobilized on beads directly bound αβ-tubulin dimers (Fig. 4 *B* and *C*). Fourth, we were unable to disrupt a complex formed between bacterially expressed MBP-Vhl and ^{35}S-labeled Mgr by adding dimeric αβ-tubulin (Fig. 4*D*). Instead the Vhl:Mgr complex also bound αβ-tubulin dimer. However, whereas *Drosophila* Vhl, like mammalian Vhl, could interact with MTs (Fig. S6 *E* and *F*), Mgr could not. This finding suggests that Mgr can interact with free, but not with polymerized, tubulin.

To test whether the interaction between Vhl and Mgr played any part in the control of tubulin degradation, we asked what the consequences would be if Mgr and Vhl were to be codepleted. *Vhl* RNAi alone had little effect on the levels of β-tubulin in cultured cells (Fig. 4 *E* and *F*), confirming the recent finding of Duchi and colleagues (19). Moreover, Vhl depletion resulted in only a slight increase in the proportion of mitotic cells with monopolar or disorganized spindles or lacking centrosomes (Fig. 4 *G*–*J*). In contrast, Mgr depletion resulted in a clear decrease in β-tubulin levels, formation of monopolar/disorganized spindles in the majority of mitotic cells, and an increase of the number of cells without centrosomes. We found all three of these phenotypes were significantly rescued by the codepletion of Vhl (Fig. 4 *E* and *J*). Thus, the proteolytic destruction of tubulin, which takes place when tubulin cannot be correctly folded by the Prefoldin chaperone, requires the function of the Vhl protein.

Discussion

The finding that the *Drosophila merry-go-round* gene encodes a subunit of the Prefoldin complex has allowed us to account for aberrant structure and function of spindles and centrosomes in cells depleted of its gene product. The inability to correctly fold tubulins in Prefoldin-deficient cells leads to tubulin instability and, hence, defects that can be phenocopied by depleting β- or γ-tubulin. However, whereas β-tubulin depletion phenocopied all of the defects observed, γ-tubulin depletion only recapitulated some of them. The more dramatic phenotypes seen in Mgr-deficient cells expressing high levels of tubulin (primary spermatocytes and neuroblasts expressing a β-tubulin transgene) suggest that the Prefoldin complex is critical to maintain tubulin levels above a certain threshold of tubulin expression. This finding could be a consequence of the impact of an excess of tubulin upon its complex folding pathway. Interestingly, in mammalian cells, increased soluble tubulin, in response to a MT-destabilizing agent, leads to the rapid degradation of tubulin (33, 34). In *Drosophila*, tubulins in the testes are the most affected by the absence of Mgr compared with other tissues. Indeed, it may be of particular importance to regulate tubulin levels at the late stages of spermatogenesis, where the very large meiotic cells are provided with proportionally large amounts of tubulin that are used in the meiotic spindle but have a major additional purpose: the building of the sperm tail. Similarly, in the mouse, the effects of depletion or mutation of prefoldin subunits are largely restricted to the brain, where tubulin levels are also very high (26, 27). Whether this tissue specificity is a consequence of tubulin levels will be an interesting question to address. Finally, our demonstration that Vhl is required for tubulin destruction in the absence of Mgr and the ability of Vhl to interact with tubulin monomers and dimers raises the possibility that its role as an E3 ubiquitin-protein ligase could come to play in regulating tubulin levels.

The idea that Vhl and Prefoldin can cooperate in regulating protein stability was also raised by Mousnier et al. (35), who identified the prefoldin subunit VBP1 as a binding partner of the HIV-1 viral integrase and suggested this mediated the interaction of the integrase with the Cul2-Vhl E3-Ubiquitin ligase. This finding led these authors to suggest a role for prefoldin at a pivotal part of the pathway that would determine whether a protein was passed on to the CCT chaperonin for folding or to the proteasome for degradation (35). Similarly, we can speculate that prefoldin as a partner of Vhl may well serve a key role in regulating the equilibrium between tubulin targeted for destruction or for folding and incorporation into MTs. The concentration of assembly-competent tubulin must be tightly controlled because it affects cytoskeletal dynamics. Vhl might contribute to this influence by an effect on MT dynamics through interaction with MAPs on the MT lattice (17, 18) and by intervening in the regulation of tubulin folding. There is growing evidence for a critical function of Vhl in stabilizing cytoplasmic MTs (16, 17) and axonemal MTs in response to levels of soluble tubulin (36). Reciprocally, MT stability can contribute to regulating levels of proteins that are targets of the Cul2-Vhl E3-Ubiquitin ligase, such as the HIF proteins, the levels of which fall when their mRNAs accumulate in cytoplasmic P-bodies for translational repression following MT disruption (37). It will be important in future to consider the roles played by the Prefoldin complex and Vhl to understand the interrelationships between the machinery regulating tubulin levels in relation to MT stability, both in normal and tumor cells.

Materials and Methods

Briefly, testes from pupae and CNS from third-instar larvae were dissected in PBS and fixed with methanol before proceeding to immunostaining. Cultured cells were pre-extracted before fixation with paraformaldehyde and immunostaining. Depletion of proteins in cultured cells was performed by transfection of dsRNA with transfast reagent. Protein extracts were obtained after homogeneization of cells, CNS or testes in lysis buffer. Protein interactions were tested in vitro using either recombinant commercially available tubulins (Cytoskeleton), proteins produced in bacteria, or proteins translated in reticulocyte lysate.

A more detailed description of gene constructs, cell culture, immunocytochemistry, dsRNA, microscopy, protein purification, Western blot analysis, in vitro binding assays, fly genetics, and primers list can be found in the *SI Materials and Methods* and Table S1.

ACKNOWLEDGMENTS. We thank Renate Renkawitz-Pohl for anti-β1- and -β2-tubulin antibodies and Matthew Savoian for the β1-tubulin construct; the E7-β-tubulin antibody was developed by Michael Klymkowsky and obtained from the Developmental Studies Hybridoma Bank developed under the auspices of the National Institute of Child Health and Human Development and maintained by the University of Iowa. We thank the Cancer Research Campaign and more recently Cancer Research United Kingdom for supporting this work.

1. Lundin VF, Leroux MR, Stirling PC (2010) Quality control of cytoskeletal proteins and human disease. *Trends Biochem Sci* 35:288–297.
2. Siegert R, Leroux MR, Scheufler C, Hartl FU, Moarefi I (2000) Structure of the molecular chaperone prefoldin: Unique interaction of multiple coiled coil tentacles with unfolded proteins. *Cell* 103:621–632.
3. Vainberg IE, et al. (1998) Prefoldin, a chaperone that delivers unfolded proteins to cytosolic chaperonin. *Cell* 93:863–873.
4. Siegers K, et al. (1999) Compartmentation of protein folding in vivo: Sequestration of non-native polypeptide by the chaperonin-GimC system. *EMBO J* 18:75–84.

5. Hansen WJ, Cowan NJ, Welch WJ (1999) Prefoldin-nascent chain complexes in the folding of cytoskeletal proteins. *J Cell Biol* 145:265–277.
6. Tsuchiya H, Iseda T, Hino O (1996) Identification of a novel protein (VBP-1) binding to the von Hippel-Lindau (VHL) tumor suppressor gene product. *Cancer Res* 56: 2881–2885.
7. Frew IJ, Krek W (2008) pVHL: A multipurpose adaptor protein. *Sci Signal* 1:pe30.
8. Frew IJ, Krek W (2007) Multitasking by pVHL in tumour suppression. *Curr Opin Cell Biol* 19:685–690.
9. Maxwell PH, et al. (1999) The tumour suppressor protein VHL targets hypoxia-inducible factors for oxygen-dependent proteolysis. *Nature* 399:271–275.
10. Lisztwan J, Imbert G, Wirbelauer C, Gstaiger M, Krek W (1999) The von Hippel-Lindau tumor suppressor protein is a component of an E3 ubiquitin-protein ligase activity. *Genes Dev* 13:1822–1833.
11. Hansen WJ, et al. (2002) Diverse effects of mutations in exon II of the von Hippel-Lindau (VHL) tumor suppressor gene on the interaction of pVHL with the cytosolic chaperonin and pVHL-dependent ubiquitin ligase activity. *Mol Cell Biol* 22:1947–1960.
12. Feldman DE, Thulasiraman V, Ferreyra RG, Frydman J (1999) Formation of the VHL-elongin BC tumor suppressor complex is mediated by the chaperonin TRiC. *Mol Cell* 4: 1051–1061.
13. Melville MW, McClellan AJ, Meyer AS, Darveau A, Frydman J (2003) The Hsp70 and TRiC/CCT chaperone systems cooperate in vivo to assemble the von Hippel-Lindau tumor suppressor complex. *Mol Cell Biol* 23:3141–3151.
14. Feldman DE, Spiess C, Howard DE, Frydman J (2003) Tumorigenic mutations in VHL disrupt folding in vivo by interfering with chaperonin binding. *Mol Cell* 12:1213–1224.
15. McClellan AJ, Scott MD, Frydman J (2005) Folding and quality control of the VHL tumor suppressor proceed through distinct chaperone pathways. *Cell* 121:739–748.
16. Thoma CR, et al. (2009) VHL loss causes spindle misorientation and chromosome instability. *Nat Cell Biol* 11:994–1001.
17. Hergovich A, Lisztwan J, Barry R, Ballschmieter P, Krek W (2003) Regulation of microtubule stability by the von Hippel-Lindau tumour suppressor protein pVHL. *Nat Cell Biol* 5:64–70.
18. Thoma CR, et al. (2010) Quantitative image analysis identifies pVHL as a key regulator of microtubule dynamic instability. *J Cell Biol* 190:991–1003.
19. Duchi S, et al. (2010) Drosophila VHL tumor-suppressor gene regulates epithelial morphogenesis by promoting microtubule and aPKC stability. *Development* 137: 1493–1503.
20. Schermer B, et al. (2006) The von Hippel-Lindau tumor suppressor protein controls ciliogenesis by orienting microtubule growth. *J Cell Biol* 175:547–554.
21. Thoma CR, Frew IJ, Krek W (2007) The VHL tumor suppressor: Riding tandem with GSK3beta in primary cilium maintenance. *Cell Cycle* 6:1809–1813.
22. Thoma CR, et al. (2007) pVHL and GSK3beta are components of a primary cilium-maintenance signalling network. *Nat Cell Biol* 9:588–595.
23. Geissler S, Siegers K, Schiebel E (1998) A novel protein complex promoting formation of functional alpha- and gamma-tubulin. *EMBO J* 17:952–966.
24. Lundin VF, Srayko M, Hyman AA, Leroux MR (2008) Efficient chaperone-mediated tubulin biogenesis is essential for cell division and cell migration in *C. elegans*. *Dev Biol* 313:320–334.
25. Gu Y, et al. (2008) Prefoldin 6 is required for normal microtubule dynamics and organization in *Arabidopsis*. *Proc Natl Acad Sci USA* 105:18064–18069.
26. Cao S, et al. (2008) Subunit 1 of the prefoldin chaperone complex is required for lymphocyte development and function. *J Immunol* 181:476–484.
27. Lee Y, et al. (2011) Prefoldin 5 is required for normal sensory and neuronal development in a murine model. *J Biol Chem* 286:726–736.
28. González C, Casal J, Ripoll P (1988) Functional monopolar spindles caused by mutation in mgr, a cell division gene of *Drosophila melanogaster*. *J Cell Sci* 89:39–47.
29. Kaltschmidt B, Glätzer KH, Michiels F, Leiss D, Renkawitz-Pohl R (1991) During *Drosophila* spermatogenesis beta 1, beta 2 and beta 3 tubulin isotypes are cell-type specifically expressed but have the potential to coassemble into the axoneme of transgenic flies. *Eur J Cell Biol* 54:110–120.
30. Kusano K, Johnson-Schlitz DM, Engels WR (2001) Sterility of *Drosophila* with mutations in the Bloom syndrome gene—Complementation by Ku70. *Science* 291:2600–2602.
31. Kemphues KJ, Raff RA, Kaufman TC, Raff EC (1979) Mutation in a structural gene for a beta-tubulin specific to testis in *Drosophila melanogaster*. *Proc Natl Acad Sci USA* 76:3991–3995.
32. Kemphues KJ, Kaufman TC, Raff RA, Raff EC (1982) The testis-specific beta-tubulin subunit in *Drosophila melanogaster* has multiple functions in spermatogenesis. *Cell* 31:655–670.
33. Caron JM, Jones AL, Kirschner MW (1985) Autoregulation of tubulin synthesis in hepatocytes and fibroblasts. *J Cell Biol* 101:1763–1772.
34. Huff LM, Sackett DL, Poruchynsky MS, Fojo T (2010) Microtubule-disrupting chemotherapeutics result in enhanced proteasome-mediated degradation and disappearance of tubulin in neural cells. *Cancer Res* 70:5870–5879.
35. Mousnier A, et al. (2007) von Hippel Lindau binding protein 1-mediated degradation of integrase affects HIV-1 gene expression at a postintegration step. *Proc Natl Acad Sci USA* 104:13615–13620.
36. Sharma N, Kosan ZA, Stallworth JE, Berbari NF, Yoder BK (2011) Soluble levels of cytosolic tubulin regulate ciliary length control. *Mol Biol Cell* 22:806–816.
37. Carbonaro M, O'Brate A, Giannakakou P (2011) Microtubule disruption targets HIF-1alpha mRNA to cytoplasmic P-bodies for translational repression. *J Cell Biol* 192: 83–99.